[4] Sterrett, J. R. and Barber, J. B., "A Theoretical and Experimental Investigation of Secondary Jets in a Mach 6 Free Stream with Emphasis on the Structure of the Jet and Separation Ahead of the Jet," *Proceedings of the AGARD Conference*, No. 4, Pt. 2, 1966, pp. 667–700l

[5] Abdelhamid, A. N. and Dosanjh, D. S., "Mach Disc and Riemann Wave in Underexpanded Jet Flows," AIAA Paper No. 69-665, San Francisco, Calif., 1969.

[6] Mirels, H. and Mullen, J. F., "Expansion of Gas Clouds and Hypersonic Jets Bounded by a Vacuum," *AIAA Journal*, Vol. 1, No. 3, March 1963, pp. 596–602.

[7] Wedemeyer, E. H., "Asymptotic Solutions for the Expansion of Gas into Vacuum," Rept. 1278, April 1965, Ballistic Research Lab., Aberdeen, Md.

[8] Hubbard, E. W., "Expansion of Uniform Gas Clouds Into a Vacuum," *AIAA Journal*, Vol. 5, No. 2, Feb. 1967, pp. 378–380.

[9] Hill, J. A. F. and Draper, J. S., "Analytical Approximation for the Flow from a Nozzle into a Vacuum," *Journal of Spacecraft and Rockets*, Vol. 3, No. 10, Oct. 1966, pp. 1552–1554.

[10] Phinney, R. E., "Internal Structure of a Free Jet," TR 67-16, Oct. 1967, Martin Marietta Corp., Baltimore, Md.

[11] Bauer, A. B., "Normal Shock Location of Underexpanded Gas-Particle Jets," *AIAA Journal*, Vol. 3, No. 6, June 1965, pp. 1187–1189.

[12] Crist, S., Sherman, P. M., and Glass, D. R., "Study of the Highly Underexpanded Sonic Jet," *AIAA Journal*, Vol. 4, No. 1, Jan. 1966, pp. 68–71.

[13] Lewis, C. H., Jr. and Carlson, D. J., "Normal Shock Location in Underexpanded Gas and Gas-Particle Jets," *AIAA Journal*, Vol. 2, No. 4, April 1964, pp. 776–777.

Reducing Ballistic Range Data for the Projectile's Drag Coefficient

C. T. Crowe*
Washington State University, Pullman, Wash.
AND
R. Carlson†
United Technology Center, Sunnyvale, Calif.

THE ballistic range has been used extensively to determine the drag coefficient of spherical projectiles.[1–3] The usual practice in data reduction has been to fit the measured times by a least-squares technique to a second- or higher-order polynominal in distance and relate the coefficients thereby obtained to the drag coefficient. In flow regimes where the drag coefficient does not vary appreciably with velocity, such as hypersonic flow, the polynominal-fit technique imposes excessive precision requirements on the measurements. It is more practical in these flow regimes to use the time-distance relation for a projectile with a constant drag coefficient and determine that value which provides the best fit with the data.

The momentum equation describing the deceleration of a projectile in a stagnant atmosphere is

$$mdV/dt = -\rho V^2 C_D A/2 \tag{1}$$

Rewriting

$$dV/dt = VdV/ds$$

and integrating the previous equation, assuming C_D is constant, yields

$$V = V_0 \exp(-\rho C_D A s/2m) \tag{2}$$

where $V = V_0$ when $s = 0$. Expressing velocity as the time derivative of distance and integrating once more gives

$$t = t_0 + [\exp(\rho C_D A s/2m) - 1]/(V_0 \rho C_D A/2m) \tag{3}$$

where t_0 is the time when $s = 0$. Nondimensionalizing this equation with respect to range distance s_R and traverse time for the projectile t_R, results in

$$\bar{t} = \bar{t}_0 + (e^{\alpha \bar{s}} - 1)/\alpha \bar{V}_0 \tag{4}$$

where

$$\alpha = \rho A C_D s_R/2m$$

and the bar designates a nondimensional quantity. Equation (4) is the relation to be used for the best fit of the time-distance data.

Two data-reduction schemes based on the preceding equations have been proposed. Seiff,[4] having noted the relationship expressed by Eq. (2), suggested that the average velocity between each pair of measuring stations be calculated and plotted vs distance on semilog coordinates. The slope of the line passing through the data points is proportional to the drag coefficient. The difficulty with this scheme is locating that point in the interval where the velocity is equal to the average velocity. Seiff recommends first assuming that the average velocity occurs at the interval's midpoint and then altering this location, using the calculated drag coefficient, until the best fit with a straight line is obtained. Obviously errors can be introduced using this computational and graphical procedure, especially if large velocity decays occur between stations.

Pitkin,[5] utilizing the relation expressed by Eq. (4), proposed that the measured times corresponding to a pair of

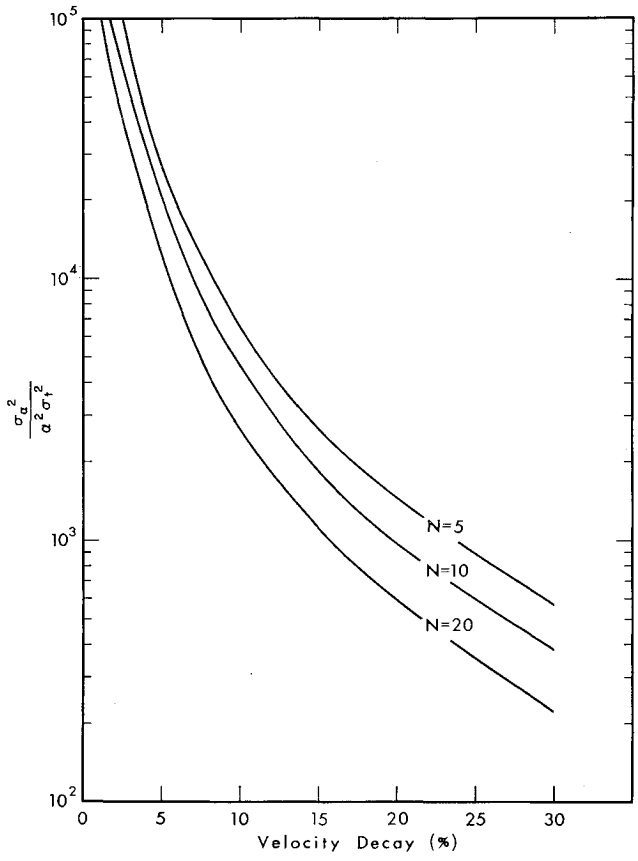

Fig. 1 Dependence of $\sigma_\alpha^2/\alpha^2\sigma_t^2$ on velocity decay and number of measuring stations.

Received December 2, 1969; revision received August 20, 1970. This work was supported in part by the U.S. Army Research Office, Durham, under contract DAH-CO4-67-C-0057.

* Associate Professor, Mechanical Engineering. Member AIAA.

† Mathematician, Physical Sciences Laboratory.

successive intervals be used to solve for the drag coefficient and velocity at the station common to both intervals. He further suggested that additional measurements be made over more intervals and the results correlated in a least-squares sense, but he made no mention how this could be done to evaluate the experimental error. The following shows how a unique fit of Eq. (4) with all the data can be achieved and the experimental error determined.

By defining a new variable

$$\eta(\alpha,s) = (e^{\alpha s} - 1)/\alpha$$

Eq. (4) can be rewritten as

$$t = t_0 + \eta(\alpha,s)/V_0 \tag{5}$$

where, for purposes of clarity, the bars designating nondimensional quantities have been deleted. It is noted that t must vary linearly with η. Choosing an arbitrary α, a least-squares fit of t with η can be established to yield t_0 and V_0, and the associated error is given by

$$\epsilon = \sum_{k=1}^{N} [t_k - t_0 - \eta(\alpha,s_k)/V_0]^2 \tag{6}$$

where t_k and s_k are time-distance data pairs and N is the number of stations including the first ($s_1 = 0$). The best fit is achieved for that α where ϵ is a minimum. This operation is easily executable with conventional high-speed computers by systematically choosing values for α, evaluating ϵ and converging on that α for which ϵ is a minimum.[6] The drag coefficient corresponding to the best fit is obtained from

$$C_D = 2m\alpha/\rho A s_R \tag{7}$$

An error in C_D accrues from errors in each of the five variables in Eq. (7). The error in each variable can be combined to determine the error in C_D by employing standard statistical procedures[7] for error propagation. The errors in m, ρ, A, and s_R can be established in the usual way by considering the accuracy of various measurements, such as, distance, pressure, temperature, and mass.

The parameter α is a function of the time-distance pairs (t_k,s_k) and errors in each contribute to an error in α. Depending on the equipment available and conditions of the experiment, the errors in distance measurements may be much less than those in time.[3,8,9] The analysis which follows applies to this case.

The variance of α is related to the variance of the time deviations ($\sigma_{t_k}^2$) about the best fit curve by[7]

$$\sigma_\alpha^2 = \sum_{k=1}^{N} (\partial\alpha/\partial t_k)^2 \sigma_{t_k}^2 \tag{8}$$

taking the time variance to be the same at all stations yields‡

$$\sigma_\alpha^2 = \sigma_t^2 \sum_{k=1}^{N} (\partial\alpha/\partial t_k)^2 \tag{9}$$

It is shown in the Appendix that the sum of the derivatives of α with respect to t_k, subject to the constraint of a minimum sum of squared deviations about the curve, is

$$\Sigma(\partial\alpha/\partial t_k)^2 = [N\Sigma\eta_k^2 - (\Sigma\eta_k)^2]V_0^2/D \tag{10}$$

where

$$D = \begin{vmatrix} \Sigma\eta_k'^2 & \Sigma\eta_k'\eta_k & \Sigma\eta_k' \\ \Sigma\eta_k'\eta_k & \Sigma\eta_k^2 & \Sigma\eta_k \\ \Sigma\eta_k' & \Sigma\eta_k & N \end{vmatrix}$$

‡ This equation is not valid in those situations in which the time measurements are not statistically independent; if time measurements at each station are made with respect to a common time reference, and not with respect to a previous measurement, Eq. (8) is valid.

and

$$\eta_k' = \partial\eta(\alpha,s_k)/\partial\alpha.$$

All the summations are performed over the same range; $k = 1$ to N. With the relation expressed by Eq. (4) when $\bar{t} - \bar{t}_0 = 1$ and $\bar{s} = 1$; namely

$$V_0 = (e^\alpha - 1)/\alpha \tag{11}$$

the normalized variance of α becomes

$$\sigma_\alpha^2/\alpha^2 = [(e^\alpha - 1)/\alpha]^2[N\Sigma\eta_k^2 - (\Sigma\eta_k)^2]\sigma_t^2/\alpha^2 D \tag{12}$$

The best estimate of the time variance is

$$\sigma_t^2 = \Sigma(t_k - t_0 - \eta_k/V_0)^2/N - 3 \tag{13}$$

where three-degrees of freedom have been removed by fitting the data with a three-parameter curve. Having determined the variance of t, the variance of α is calculated by Eq. (12) and related to the error in α (and C_D) using the t probability distribution.[10]

As stated previously, this analysis is valid for the case in which errors in distance measurements are much smaller than those in time. An analysis identical to that just mentioned can be carried out for the converse case of less accurate distance measurements. If the time and distance errors are of the same order of magnitude, the more complicated bivariate regression analysis is necessary.

As an application of the preceding analysis, consider a ballistic range with N equally spaced measuring stations. The dependence of $\sigma_\alpha^2/\alpha^2\sigma_t^2$ on the velocity decay for 5, 10, and 20 measuring stations is illustrated in the accompanying figure. As anticipated a smaller $\sigma_\alpha^2/\alpha^2\sigma_t^2$ is achieved by allowing larger velocity decays or using more measuring stations.

This figure can be used to assess the error in α for a given error in time measurements. Consider the following example. A 200-ft ballistic range is used to measure the drag coefficient of a projectile moving at 5000 ft/sec. The range has ten measuring stations and the times of projectile passage are measured to within ± 1 μsec. Thus the nondimensional standard deviation of the time measurements will be of the order of 5×10^{-5}. It is assumed, of course, that the location of measuring stations is measured with more precision than the times of projectile passage.

Assume the velocity decays 10%. From the figure it is found that the variance of α is related to the variance of t by

$$\sigma_\alpha^2/\alpha^2 = 4.6 \times 10^3 \sigma_t^2$$

Thus one concludes

$$\sigma_\alpha^2/\alpha^2 < 1.2 \times 10^{-5}$$

From the tabulated values for the Student t distribution[10] for 7-degrees of freedom and a 90% confidence level, it is found

$$\Delta\alpha = \pm 1.9\sigma_\alpha/N^{1/2} \tag{14}$$

where $\Delta\alpha$ is the uncertainty in α. Substituting the aforementioned values into Eq. (14) gives

$$\Delta\alpha/\alpha < \pm 2.1 \times 10^{-3}$$

and thus shows that the error in α, as a result of errors in time measurement, will be less than $\pm 0.21\%$ with a 90% confidence level. If the conventional polynominal fit were used for the data, it can be shown that the errors in time measurement would effect an order-of-magnitude larger error in α.

The utility of the preceeding analysis in experiment design and data analysis is obvious.

Appendix

The curve to which the data are fitted is

$$t = t_0 + \eta(\alpha,s)/V_0 \tag{A1}$$

and the best fit is obtained when

$$\Sigma[t_k - t_0 - \eta(\alpha,s_k)/V_0]^2 = \text{minimum}\S \quad \text{(A2)}$$

Let δt_k represent the arbitrary deviation of a time measurement from the best-fit curve. The parameters describing the curve must change accordingly but in such a way that the sum of the squares of deviations from the curve is a minimum, i.e.,

$$\Sigma[t_k - t_0 - \delta t_0 - \delta\alpha(\partial\eta_k/\partial\alpha)/V_0 - \eta_k/V_0 - \eta_k\delta(1/V_0)]^2 = \min \quad \text{(A3)}$$

or

$$\Sigma[\delta t_\pi - t_{ck} - \delta t_0 - \eta_k'\delta\alpha/V_0 - \eta_k\delta(1/V_0)]^2 = \min \quad \text{(A4)}$$

where t_{ck} is the time given by the best-fit curve (Eq. A1) at station k. Taking the derivative of Eq. (A4) with respect to δt_0, $\delta\alpha$, and $\delta(1/V_0)$ and equating each to zero yields a set of three equations for δt_0, $\delta\alpha$, and $\delta(1/V_0)$ as a function of δt_k. Taking the derivative of each equation with respect to δt_k produces the following set of equations for $\partial t_0/\partial t_k$, $\partial\alpha/\partial t_k$, and $\partial(1/V_0)/\partial t_k$

$$\begin{aligned}
\eta_k'/V_0 &= (\partial\alpha/\partial t_k)\Sigma\eta_k'^2/V_0^2 + [\partial(1/V_0)/\partial t_k]\,\Sigma\eta_k\eta_k'/V_0 + (\partial t_0/\partial t_k)\Sigma\eta_k'/V_0 \\
\eta_k &= (\partial\alpha/\partial t_k)\,\Sigma\eta_k\eta_k'/V_0 + [\partial(1/V_0)/\partial t_k]\,\Sigma\eta_k^2 + (\partial t_0/\partial t_k)\,\Sigma\eta_k \quad \text{(A5)} \\
1 &= (\partial\alpha/\partial t_k)\,\Sigma\,\eta_k'/V_0 + [\partial(1/V_0)/\partial t_k]\,\Sigma\eta_k + (\partial t_0/\partial t)_k N
\end{aligned}$$

Solving for $\partial\alpha/\partial t_k$, squaring and summing over k gives

$$\Sigma(\partial\alpha/\partial t_k)^2 = [N\Sigma\eta_k^2 - (\Sigma\eta_k)^2]V_0^2/D \quad \text{(A6)}$$

where

$$D = \begin{vmatrix} \Sigma\eta_k'^2 & \Sigma\eta_k'\eta_k & \Sigma\eta_k' \\ \Sigma\eta_k'\eta_k & \Sigma\eta_k^2 & \Sigma\eta_k \\ \Sigma\eta_k' & \Sigma\eta_k & N \end{vmatrix}$$

References

[1] Hodges, A. J., "The Drag Coefficient of Very High Velocity Spheres," *Journal of Aeronautical Sciences*, Vol. 24, No. 10, Oct. 1957, pp. 755–758.

[2] May, A. and Witt, W. R., "Free Flight Determination of the Drag Coefficients of Spheres," *Journal of Aeronautical Sciences*, Vol. 20, No. 9, Sept. 1953, pp. 635–638.

[3] Charters, A. C. and Thomas, R. N., "The Aerodynamic Performance of Small Spheres from Subsonic to High Supersonic Velocities," *Journal of Aeronautical Sciences*, Vol. 12, No. 4, Oct. 1945, pp. 468–476.

[4] Seiff, A., "A New Method for Computing Drag Coefficients from Ballistic Range Data," *Journal of Aeronautical Sciences*, Vol. 25, No. 2, Feb. 1958, pp. 133–134.

[5] Pitkin, E. T., "Determination of Flight Speeds and Drag Coefficients from Time and Distance Measurements," *Journal of Spacecraft and Rockets*, Vol. 5, No. 8, Aug. 1968, pp. 1000–1002.

[6] Bevington, P. R., *Data Reduction and Error Analysis for the Physical Sciences*, McGraw-Hill, New York, 1969, pp. 204–246.

[7] Baird, D. C., *Experimentation: An Introduction to Measurement Theory and Experiment Design*, Prentice Hall, Englewood Cliffs, N.J., 1968, p. 63.

[8] Crowe, C. T. et. al., "Measurement of Particle Drag Coefficients in Flow Regimes Encountered by Particles in a Rocket Nozzle," 2296-FR, Contract No. DAH-C04-67-C-0057, March 1969, United Technology Center, Sunnyvale, Calif.

[9] Slattery, J. C., Friichtenicht, J. F., and Hamermesh, B., "Interaction of Micrometeorites with Gaseous Targets," *AIAA Journal*, Vol. 2, No. 3, March 1964, pp. 543–548.

[10] Fraser, D. A. S., *Statistics, An Introduction*, Wiley, New York, 1958, p. 389.

§ All summations are performed from $k = 1$ to $k = N$.

A Comparison of Boundary-Layer Transition Data from Temperature-Sensitive Paint and Thermocouple Techniques

GEORGE G. MATEER*

NASA Ames Research Center, Moffett Field, Calif.

Nomenclature

M = Mach number
p = pressure
u = velocity
s = distance along model surface from nose
T = temperature
ρ = density
μ = viscosity

Subscripts

e = boundary-layer edge condition
t = total condition
∞ = freestream condition

REFERENCES 1 and 2 demonstrated that the phase-change, temperature-sensitive paint technique is a reliable method for obtaining quantitative aerodynamic heating data. In Ref. 2, these data were used as an indicator of boundary-layer transition, and transition Reynolds numbers were compared with those from other investigations. However, an assessment of the method for quantitative measurements of transition could not be made from this comparison because of differences in transition data between facilities. Since the simplicity of the technique would make it particularly suited for transition studies on complex configurations, a study was made to determine whether the temperature-sensitive paint technique would yield the same quantitative results as more conventional methods.

Tests were conducted in the Ames Research Center's 3.5-ft hypersonic wind tunnel on 5° half-angle cones at a freestream Mach number of 7.4. The total temperature was nominally 1500°R and total pressures ranged from 200 to 1800 psia, accordingly, freestream unit Reynolds numbers varied from 0.9 to 8 × 10^6/ft. Boundary-layer transition was determined from heat-transfer distributions obtained by the temperature-sensitive paint and from the thermocouple-calorimeter techniques. The thermocouple tests have been previously reported.[3] For the paint tests the model was 22.75 in. long and a paint was selected that changed phase (solid to liquid) at 200°F. Heating rates were deduced from photographs of the melt line as described in Ref. 1.

An example of heating-rate data is shown in Fig. 1. Paint and thermocouple data compare very well over the entire boundary layer (laminar, transitional, and turbulent). The

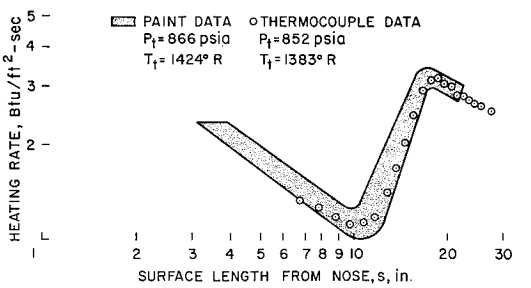

Fig. 1 Comparison of heating rates on 5° half-angle cones at M_∞ = 7.4.

Received August 13, 1970.

* Research Scientist. Associate Member AIAA.